Ferrofluids: flexibility of magnetic particle chains

2004 J. Phys.: Condens. Matter 16 3807

(http://iopscience.iop.org/0953-8984/16/23/001)

INSTITUTE OF PHYSICS PUBLISHING JOURNAL OF PHYSICS: CONDENSED MATTER

J. Phys.: Condens. Matter **16** (2004) 3807–3818 PII: S0953-8984(04)76207-4

Ferrofluids: flexibility of magnetic particle chains

Konstantin I Morozov[1] **and Mark I Shliomis**[2]

[1] Institute of Continuous Media Mechanics, UB of Russian Academy of Sciences, 614013 Perm, Russia
[2] Department of Mechanical Engineering, Ben-Gurion University of the Negev, POB 653, Beer-Sheva 84105, Israel

E-mail: mrk@icmm.ru and shliomis@bgu.ac.il

Received 10 February 2004
Published 28 May 2004
Online at stacks.iop.org/JPhysCM/16/3807
DOI: 10.1088/0953-8984/16/23/001

Abstract

Conformational properties of dipolar chains, and spatial and orientational intra-chain correlations in zero and infinitely strong external fields are investigated theoretically. A striking similarity and essential distinctions between the chains and polymer molecules are revealed and discussed. The main attention is given to the chain flexibility. The coil–globule phase transition in dipolar chains is predicted.

1. Introduction

Fluid of dipolar hard spheres is the basic model in statistical mechanics of polar liquids. An important 'natural' representative of dipolar fluids is *ferrofluids* (FF) [1, 2]—the colloidal solutions of magnetic grains. The distinctive and attractive features of FF are due to the presence of two control parameters: the particle size (it determines the scale of interparticle interactions) and the concentration. An excess of anisotropic dipole interactions over energy of thermal fluctuations leads to the formation of *chains* out of head-to-tail aligned magnetic dipoles. This was a surprising result of Monte Carlo simulations [3–7]. Many intriguing and unexpected properties of FF established during last decade are due to the chains. To all appearances, the chain formation precedes the gas–liquid *phase separation* formerly predicted analytically [8] (within the limits of the *mean spherical model* [9]) and recently observed in simulations [10]. The two effects are divided by their scales: the condensation manifests as *macroscopic* phenomenon whereas the chain formation manifests as a *microscopic* one. The pathway between the phenomena was given in the recent Monte Carlo study [11, 12] of gas–liquid nucleation in a strongly polar Stockmayer fluid. As shown, the nucleation is initiated by chains which then grow in length and finally collapse to spherical clusters as the result of *coil–globule* transition.

Theoretical investigations of association phenomena in FF started from pioneering works of de Gennes and Pincus [13] and Jordan [14]. The latter treated FF as a chemical equilibrium

mixture of non-interacting clusters of different size. This reasonable approach became the basis for latest theoretical works [15–22]. So, combining the van der Waals theory for liquid condensation with the associated Jordan theory revealed [15] a competition between liquid condensation and chain formation in accordance with mentioned simulations [3–7]. Analogous results were obtained in [16–19] where some phenomenological parameters of work [15] were estimated.

Remarkably, all of the aforementioned theoretical works dealt with only one attribute of dipolar chains—their length. Meanwhile, a genuine understanding of the phenomenon remains incomplete without studying the *spatial* and *orientational* correlations along the chain. Investigating these correlations, we have established an important role of the chain *flexibility*: this property of chains has never been the subject of study. De Gennes and Pincus [13] were the first who noted an analogy between dipolar chains and polymer molecules. In fact, developing the association theory, we arrive at a natural extension of basic concepts of polymer physics (such as a coil, globule, the persistent length, Kuhn's segment etc [23]) to the case of dipolar chains. Below we study possible *conformations* of the chains (statistical coil, globule) and investigate the coil–globule phase transition.

2. Factorization of the partition function of ideal chain

Consider FF as an assembly of chains of different length formed out of magnetic grains. We assume that all the grains are identical spheres of diameter d, only neighbouring grains in the chain interact with each other, and there is no interaction between grains of different chains. In other words, we consider for the moment a case of *ideal* chains.

The grain interaction is described by the sum of hard-sphere $U_{\rm hs}(r)$ and dipolar potentials,

$$U(12) = U_{\rm hs} - (m^2/r^3)\left[3(\mathbf{e}_1\cdot\hat{\mathbf{r}})(\mathbf{e}_2\cdot\hat{\mathbf{r}}) - \mathbf{e}_1\cdot\mathbf{e}_2\right], \tag{1}$$

where $\mathbf{e}_i$ and $\hat{\mathbf{r}}$ are unit vectors along the magnetic moment of a particle i, $\mathbf{m}_i = m\mathbf{e}_i$, and along the interparticle vector $\mathbf{r}_{12} = r\hat{\mathbf{r}}$.

We give a definition to the chain. First, two neighbouring grains are reputed to be bonded if their dipolar potential for the head-to-tail dipole configuration exceeds thermal energy, $2m^2/r^3 \geqslant k_{\rm B}T$. Other words, the distance r between the grains should satisfy the condition $r^3 \leqslant 2\lambda d^3$ where $\lambda = m^2/(d^3 k_{\rm B}T)$ is the dimensionless coupling parameter. Second, calculating the partition function Z_N of an N-particle chain, the integration over displacement vector $\mathbf{r}_{i,i+1}$ of two neighbouring particles should be done over *half* the spherical volume admitted by the above mentioned condition.

Let us comment on the last statement. The procedure of integration was proposed in [22]. It allows us, effectively, to take into account the steric interactions with other grains in a chain. Of course, the given integration narrows down the real region of space admitted for the particle in a chain. However, it contains the main region around the head-to-tail configuration of dipoles. The results of exact integration and integration over half the spherical volume prove to be practically coincide starting from $\lambda \geqslant 3$, that is from the same beginning of the grain association as we will see later. In order to show the chosen method of integration over half the spherical layer we use below the prime near the symbol of integral.

The main advantage of the model is *factorization* of the partition function of an N-particle chain: $Z_N = Z_2^{N-1}$ where Z_2 is the partition function of a *dimer*—the cluster of two grains. Such a factorization takes place in either zero or infinitely strong magnetic fields, but not for arbitrary external field strength. This property of a dipolar chain is quite analogous to that for the chain of spins with the Heisenberg interactions [24]. In zero field it immediately follows from the absence of a preferable direction in the system. So, calculating Z_N one should

integrate over variables $\mathbf{e}_i$ and $\mathbf{r}_{i-1,i}$ starting from the last grain of number N ('tail' of the chain) to the first one ('head') and taking at each step the direction $\mathbf{e}_{i-1}$ of the previous grain for the polar axis. In the case of infinitely strong field, the factorization is obvious. As soon as Z_N is known, the chain distribution upon their length is easily calculated (see, e.g., [14, 15, 18, 19]). In particular, the average number of grains in the chain is

$$\langle N\rangle = \tfrac{1}{2} + \sqrt{\tfrac{1}{4} + \Phi Z_2}, \tag{2}$$

where $\Phi = nv$ is the volume fraction of magnetic particles, and n and $v = \pi d^3/6$ are their concentration and volume, respectively.

Thus the problem of determination of the average length of the chains is reduced to calculation of the partition function of dimer. The asymptotic representation at $\lambda \gg 1$ of the dimer partition function in zero and infinite external field is calculated in detail in the appendix. The result is

$$Z_2(0) = \frac{\mathrm{e}^{2\lambda}}{3\lambda^3}\left(1 + \frac{8}{3\lambda} + \frac{23}{3\lambda^2} + \frac{229}{9\lambda^3} + \frac{5263}{54\lambda^4} + \frac{11\,536}{27\lambda^5} + \frac{57\,427}{27\lambda^6}\right), \tag{3}$$

$$Z_2(\infty) = \frac{\mathrm{e}^{2\lambda}}{3\lambda^2}\left(1 + \frac{5}{3\lambda} + \frac{41}{12\lambda^2} + \frac{155}{18\lambda^3} + \frac{11\,195}{432\lambda^4} + \frac{39\,235}{432\lambda^5} + \frac{628\,145}{1728\lambda^6}\right). \tag{4}$$

These expansions are given up to terms of order of $\mathrm{O}(\lambda^{-6})$ because of the slow convergence of the series. The main (first) term in the right side of (3) and (4) is a result of de Gennes and Pincus [13]. The calculated values of both partition functions are shown in figure 1; note that in the figure and below, the minimal value of λ is 0.5 according to our definition of a chain. It is interesting that maximal deviations of calculated values from unity (i.e. from de Gennes and Pincus asymptotic values) takes place at small $\lambda \sim 2{-}3$, however even at $\lambda = 10$ it achieves 50%. The expansions (3) and (4) describe the calculated values within the accuracy of 10% starting from $\lambda \sim 6$.

Being the very important integral characteristic of the phenomenon of chain formation, the average length itself, however, does not contain an exhaustive information about the system. Our understanding of the phenomenon would be incomplete without study of *statistical properties* of the chains, including their spatial and orientational correlations. It is these questions we start to investigate.

3. Statistical properties of ideal chains

We study now the statistical properties of a *single chain*. Owing to the factorization, the problem again reduces to study of statistical properties of nothing but dimers. The properties are expressed through four orientational and two spatial correlation functions:

$$\begin{aligned} &A = \langle \mathbf{e}_1 \cdot \mathbf{e}_2\rangle, \qquad B = \langle \mathbf{e}_1 \cdot \mathbf{r}_{12}\rangle d^{-1}, \qquad C = \langle (\mathbf{e}_1 \cdot \mathbf{e}_2)^2\rangle, \\ &D = \langle (\mathbf{e}_1 \cdot \mathbf{r}_{12})^2\rangle d^{-2}, \qquad E = \langle r_{12}\rangle d^{-1}, \qquad F = \langle r_{12}^2\rangle d^{-2}. \end{aligned} \tag{5}$$

All of them depend only on λ and are easily calculated. We determined also their asymptotic representation at $\lambda \gg 1$ which is given in the appendix. Note that even for strong dipole interactions, $\lambda = 10$, these correlations are still far from unity. For example, the mean values of cosine $(\mathbf{e}_1 \cdot \mathbf{e}_2)$ and its square are (see equations (A.12) and (A.18)): $A \approx 0.77$ and $C \approx 0.64$. This means that orientations of neighbouring dipoles preserve a fairly high rotational mobility inside dimers.

The dimer correlations (5) contain *all* necessary information about the chain. For instance, the correlation in orientations of i and $i+k$ dipoles pertaining to the same chain is multiplicative, $\langle \mathbf{e}_i \cdot \mathbf{e}_{i+k}\rangle = A^k$, and then decays exponentially. Hence, using a polymeric analogy [23], one can

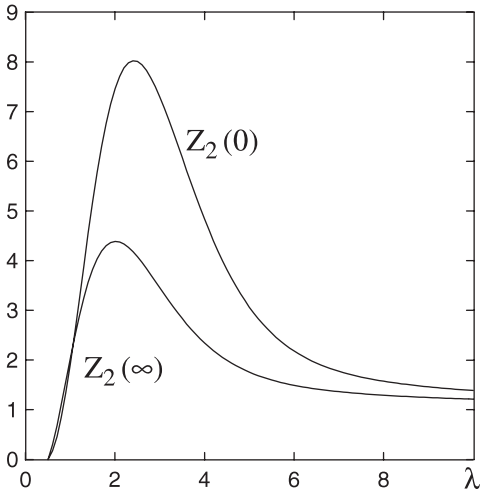

Figure 1. The partition functions of dimer in zero and infinite external fields in units of de Gennes and Pincus asymptotic values $\exp(2\lambda)/3\lambda^3$ and $\exp(2\lambda)/3\lambda^2$, respectively.

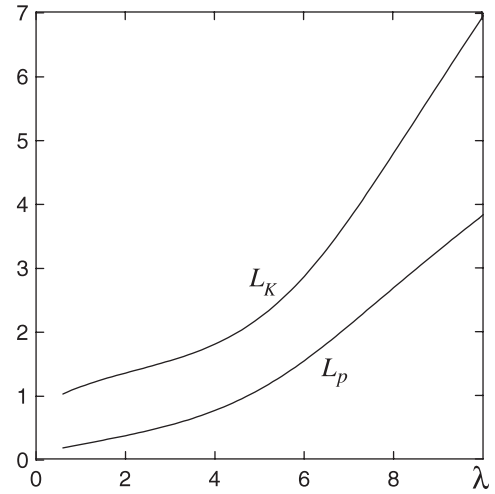

Figure 2. The persistence L_p and Kuhn L_K lengths versus the coupling parameter λ.

introduce the *persistence length* $L_\mathrm{p} = -E/\ln A$ (in units of particle diameter d) characterizing the chain flexibility. This quantity is shown in figure 2. For $\lambda \gg 1$ there is

$$L_\mathrm{p} = \frac{\lambda}{2} - \frac{11}{12} - \frac{23}{18\lambda} - \frac{128}{27\lambda^2} - \frac{9698}{405\lambda^3} - \frac{1423\,259}{9720\lambda^4}. \tag{6}$$

As in the case of the partition functions (3) and (4), this expansion well describes (within the accuracy of a few per cent) the calculated values of L_p starting from $\lambda \geqslant 6$. For $\lambda = 12.25$, it gives $L_\mathrm{p} = 5.1$ as opposed to $L_\mathrm{p} \simeq 7$ obtained in the simulation [7]. Thus, dipolar chains are very flexible: only on scales not exceeding $\lambda d/2$ may they be considered as rigid.

The most informative quantity of chain conformation is the 'end-to-end' vector $\mathbf{R} = \sum_{i=1}^{N-1} \mathbf{r}_{i,i+1}$ connecting centres of the first and last particles in a chain. We have calculated $\langle R^2\rangle = \langle R_\parallel^2\rangle + 2\langle R_\perp^2\rangle$ where $\parallel$ means 'along $\mathbf{e}_1$' and $\perp$—the perpendicular direction. The result is expressed via the dimer's mean values (5):

$$\begin{aligned} \frac{\langle R^2\rangle}{d^2} &= F(N-1) + \frac{2AB^2}{1-A}\left[N - 2 - AP_{N-2}(A)\right], \\ \frac{\langle R_\parallel^2\rangle - \langle R_\perp^2\rangle}{d^2} &= \frac{3D-F}{2}P_{N-1}(G) + \frac{2AB^2}{A-G}\left[AP_{N-2}(A) - GP_{N-2}(G)\right], \end{aligned} \tag{7}$$

where $G = (3C-1)/2$ and $P_N(x) = (1-x^N)/(1-x)$. For dimers, $N = 2$, the obvious result $\langle R_\parallel^2\rangle = Dd^2$, $\langle R_\perp^2\rangle = (F-D)d^2/2$ is recovered. For very short chains, $N \ll \lambda$, we have $\langle R_\parallel^2\rangle = N^2d^2$ and $\langle R_\perp^2\rangle = 0$, which is just the case of *rod-like* aggregates claimed to exist by Zubarev and Iskakova [21, 22]. However, according to equation (2) the mean number of grains in a chain $\langle N\rangle$ grows with λ so quickly ($\propto \mathrm{e}^\lambda$) that the condition $\langle N\rangle \ll \lambda$ is *never satisfied*. Therefore, although statistically some number of such short chains still exists, their fraction is negligible [3–6, 16, 18].

For a long chain, $N \gg \lambda$, equation (7) gives $\langle R_\perp^2\rangle = \langle R_\parallel^2\rangle$: the chain forms a *spherical coil*. Its mean-squared end-to-end distance is proportional to N as typical of ideal polymer chain [23]:

$$\langle R^2\rangle = Nd^2[F + 2AB^2/(1-A)]. \tag{8}$$

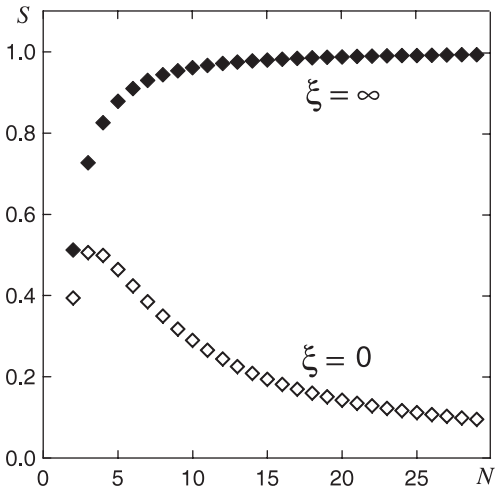

Figure 3. Non-sphericity parameter S as a function of number of particles in a chain in zero (open diamonds) and infinite (full diamonds) external field. The coupling parameter $\lambda = 10$.

The chain *stiffness* is commonly characterized (along with the persistent length L_p) by the *Kuhn segment* L_K. This is determined by the relation $\langle R^2 \rangle = N\langle r \rangle L_K d$ where $\langle r \rangle$ is the mean distance between neighbouring grains in the chain. Both the quantities, L_K and L_p, are depicted in figure 2 as functions of λ. Interestingly, starting from $\lambda \simeq 5$ (i.e. when the aggregation phenomenon becomes sufficiently appreciable) the ratio L_K/L_p proves to be close to 2 as it takes place for many models of polymer molecules [23]. Note that the linear (along the chain) memory disappears at the distances of only a few grains.

Chains of a *finite* length form statistical coils whose shape deviates from spherical. The deviation may be characterized by the parameter of non-sphericity $S = (\alpha^2 - \beta^2)/(\alpha^2 + \beta^2)$ where $\alpha = d + \langle R_\parallel^2 \rangle^{1/2}$ and $\beta = d + \langle R_\perp^2 \rangle^{1/2}$ are the chain scales in two directions. As seen from figure 3, in the absence of magnetic field, S quickly decreases with increasing N. For a strong dipole interaction ($\lambda \simeq 10$) and the volume fraction of magnetic particles $\phi \sim 0.01$, equations (2) and (3) give $\langle N \rangle \simeq 50$. So, once more we conclude that the chain of magnetic grains is a flexible formation with a short persistent length ($L_p \simeq 5$). Such a chain resembles a *cloud* or *coil* of connected monomers and has quasi-spherical form.

Insert now the ferrofluid in an infinitely strong magnetic field. As noted above, in such a field the factorization of the problem takes place as well as in zero field, thus the general result (7) remains valid. At $\xi \to \infty$ the dimer correlations A_∞, B_∞, etc, differ of course from their zero-field values; e.g., evidently, $A_\infty = C_\infty = 1$. Then equation (7) yields the characteristic size of chains along the field and in the perpendicular direction:

$$\begin{aligned} \langle R_\parallel^2 \rangle / d^2 &= (N-1)\left[B_\infty^2 (N-2) + D_\infty\right], \\ \langle R_\perp^2 \rangle / d^2 &= (N-1)(F_\infty - D_\infty)/2. \end{aligned} \tag{9}$$

Thus, the length of a long chain increases $\propto N$ along the field, while the transverse size remains of the order of $\sqrt{N}$. The non-sphericity S drastically increases with N and quickly approaches unity—see figure 3.

The proposed representation of magnetic fluid as an assembly of ideal flexible chains admits a straightforward calculation of *macroscopic* properties of the system. For instance, the initial magnetic susceptibility χ is expressed compactly via its Langevin value $\chi_L = nm^2/3k_BT$, the correlation function A, and the average chain length $\langle N \rangle$ (see

equation (2)) as

$$\chi = \chi_{\rm L}\frac{1 + A(1 - 1/\langle N\rangle)}{1 - A(1 - 1/\langle N\rangle)}. \tag{10}$$

In the limit $\lambda \gg 1$ when $\langle N\rangle \gg 1$ and $A \approx 1 - 2\lambda^{-1} - 2\lambda^{-2}$ (see equation (A.12)), the last expression takes the form $\chi \approx (\lambda - 2)\chi_{\rm L}$. The important peculiarity of the relation is the dependence of susceptibility χ on both dipolar parameters—$\chi_{\rm L}$ and λ. The former characterizes the mean dipolar interaction in the system (note that majority of theories describes χ using only this interaction parameter [25]). The latter accounts for the short-range effects of cluster formation when two grains are in contact with each other. In spite of an elegant form of expression (10) we however do not proceed to its physical consequences. The point is that this equation has been found for the case of *ideal* chains. As we will see in the next section an account of non-neighbouring grain interactions leads to the transformation of a friable coil into a dense globule that makes the result (10) practically useless.

4. Nonideal chains. The coil–globule transition

Above we make allowance for interactions of only neighbouring grains belonging to the same chain ignoring interactions between (i) the non-nearest neighbours along the chain, (ii) the distant segments of the same chain which are found near each other owing to chain flexibility, and (iii) the segments of different chains. The account of the first of them in the case of straight linear chains reduces [14] to the simple re-normalization of the nearest-neighbours interactions: $\lambda \to \lambda\zeta(3)$ where $\zeta(3) = 1.202$ is the Riemann ζ-function. The chain flexibility should only decrease this value, thus the point (i) may be regarded as insignificant. The second type of interactions can form antiparallel side-by-side configurations of dipoles in zero field. The third type should be taken into account along with the second because the friable coils of ideal chains (with typical volume of $\propto N^{3/2}$ in zero field) begin to overlap already at small volume fractions ($\phi \leqslant 1$) of magnetic grains. A due regard for these interactions can be carried out in the frame of the concept of *quasi-monomers* [23] treating a long flexible chain as a system of *disconnected* segments. For the sake of simplicity, we identify each a segment with an *individual* grain and make allowance for interactions between the segments in the approximation of the second virial coefficient $b_{\rm seg}$. Let us calculate it.

At first, write down the usual second virial coefficient of free dipoles b_2 scaled by the grain volume v:

$$b_2 = -\frac{1}{2v}\int_V \mathcal{F}(12)\,f(1)\,f(2)\,{\rm d}\mathbf{e}_1\,{\rm d}\mathbf{e}_2\,{\rm d}\mathbf{r}, \tag{11}$$

where V is the volume of an ellipsoidal container filled with FF, $\mathcal{F}(12) = \exp(-U(12)/k_{\rm B}T) - 1$ is the Mayer function with the potential (1), $f(i) = (\xi/4\pi\sinh\xi)\exp(\xi\,\mathbf{e}_i\cdot\mathbf{h})$ is the one-particle orientational distribution function in the field $\mathbf{H} = H\mathbf{h}$. It should be noted that calculating the second virial coefficient there is no need to distinguish the external and internal magnetic fields: the difference between them takes place in higher orders of grain concentration.

Following to Kirkwood's idea [26], we put the particle 1 in the centre of a spherical volume $v_* = 4\pi r_*^3/3$, outside which interparticle interaction is weak: $U(12) \leqslant k_{\rm B}T$ for $r \geqslant r_*$. Then b_2 is decomposed onto three terms:

$$\begin{aligned} &b_2 = b_{\rm hs} + b_{\rm mag} + b_{v_*}: \qquad b_{\rm hs} = 4, \qquad b_{\rm mag} = 12\lambda\left(n_{\rm s} - \tfrac{1}{3}\right)L^2(\xi),\\ &b_{v_*} = -\frac{1}{2v}\int_{v_*}\mathcal{F}(12)\,f(1)\,f(2)\,{\rm d}\mathbf{e}_1\,{\rm d}\mathbf{e}_2\,{\rm d}\mathbf{r}, \end{aligned} \tag{12}$$

where $L(\xi) = \coth\xi - 1/\xi$ is the Langevin function of the dimensionless field strength $\xi = mH/k_BT$ and n_s is the demagnetizing factor of the sample. The *hard-spheres* repulsion contributes the value $b_{hs} = 4$, while the field dependent term $b_{mag} \propto L^2(\xi)$ is an inevitable consequence of the long-range nature of dipolar interactions [13]. Integration in the last term is performed over the spherical layer $d \leqslant r \leqslant r_*$.

The next step is accounting for the difference between virial coefficients of quasi-monomers b_{seg} and free dipoles b_2. The difference originates just from the chain flexibility, owing to which two segments being far apart along the chain can prove to be at a short distance. Other words, b_{seg} is due to interaction of grains belonging to *different* Kuhn segments. Two grains are reputed to belong to the same segment if inclination of $\mathbf{e}_1$ and $\mathbf{e}_2$ to the displacement vector $\mathbf{r}$ does not exceed 60°. In the opposite case, particles 1 and 2 belong to different segments. Naturally, the configuration space of quasi-monomers is smaller than that of a pair of free dipoles. To make allowance for that fact, one should introduce in the last term in (11) the cutoff factors $\Theta(\frac{1}{2} - |\mathbf{e}_i \cdot \hat{\mathbf{r}}|)$; the Heaviside step-function $\Theta(x)$ differs from zero only for $x > 0$. Then we finally have

$$b_{seg} = 4 + 12\lambda\left(n_s - \tfrac{1}{3}\right)L^2(\xi) - \frac{1}{2v}\int_{v_*} \mathcal{F}(12) f(1)\Theta\left(\frac{1}{2} - |\mathbf{e}_1 \cdot \hat{\mathbf{r}}|\right) f(2)\Theta\left(\frac{1}{2} - |\mathbf{e}_2 \cdot \hat{\mathbf{r}}|\right) \mathrm{d}\mathbf{e}_1\, \mathrm{d}\mathbf{e}_2\, \mathrm{d}\mathbf{r}. \quad (13)$$

Now we intend, using the second virial coefficient of quasi-monomers (13), to judge what interaction—repulsive or attractive—prevails in the system. If the potential of interaction is *short-range*, we would apply the usual condition $b_{seg} = 0$. In the theory of polymer solutions, this relation determines the so-called 'theta temperature' [23]. However, our situation is more complicated due to *long-range* dipolar interaction. The result of dipolar interaction is the appearance of a shape-dependent term b_{mag} in equations (12) and (13). The physical meaning of such a term becomes clear writing the corresponding contribution into volume density of free energy of the system:

$$F_{mag} = k_BT b_{mag} v n^2 = 2\pi(n_s - \tfrac{1}{3})M^2, \quad (14)$$

where $M = nmL(\xi)$ is the ferrofluid magnetization. From here F_{mag} is identified as *magnetostatic energy* of a macroscopically homogeneous sample. We emphasize that this term is due only to long-range effects. It forms the long-range 'background' for the short-range effects. Therefore, to judge the short-range effects, we should exclude the 'background', i.e. one should consider b_{mag} as a *reference point* for the second virial coefficient b_{seg}. In other words, for the dipolar system the mentioned condition of balance of attractive and repulsive forces takes the form

$$\Delta b_{seg} = b_{seg} - b_{mag} = 0; \quad (15)$$

and, apparently, Δb_{seg} is shape-independent.

Calculate now when Δb_{seg} take zero values. We choose the radius r_* from the natural limitation $m^2/r_*^3 = k_BT$: the potential of *side-by-side* dipole orientations must not exceed thermal energy within the sphere $r \leqslant r_*$. Then we find Δb_{seg} as a function of the inverse temperature λ and the field ξ. The condition $\Delta b_{seg}(\lambda, \xi) = 0$ determines the *neutral curve* $\lambda_c(\xi)$ shown in figure 4. Lower in this curve, where steric repulsion prevails over magnetic attraction ($\Delta b_{seg} > 0$), dipolar chains exist in the form of *coils* in zero and weak magnetic fields ($\xi \ll 1$) or almost straight stripes along the strong field ($\xi \gg 1$). Vice versa, higher in the curve, where attraction predominates ($\Delta b_{seg} < 0$), the coil-like chains become *unstable* and collapse into dense *globules* or, probably, into an extended network [27]. Although the curve cannot be precise for small λ because of the small length of the chains

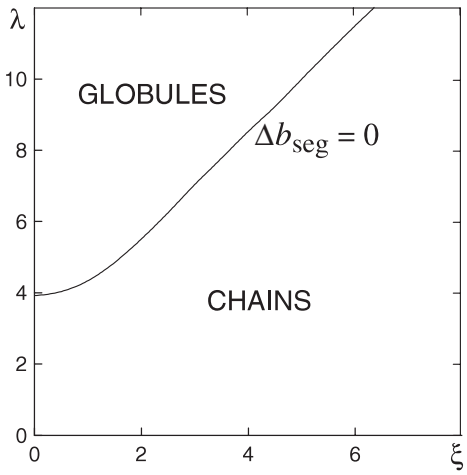

Figure 4. Line of coil–globule transition in the plane of coupling parameter λ—field ξ.

according to equation (2) and figure 1, the value $\lambda_c(0) = 3.9$ is reasonably less than the inverse critical temperature $\lambda_*(0) = 4.45$ for the gas–liquid phase separation [8]. Indeed, globule formation should *precede* the separation. Just that very pathway was revealed in the Monte Carlo study of a polar Stockmayer liquid [11]: the globules were the *nuclei* of future condensation.

We make in conclusion some remarks about the validity of our approximation. As seen from (13), nearby the neutral curve $\Delta b_{\rm seg} \sim 1$. Therefore, as long as we are interested in the *onset* of coil–globule transition rather than in the low-temperature globular state itself, the second virial coefficient approximation is certainly valid. Its validity for *interchain* interactions is limited by the condition $\phi \ll 1$. Hence the term $\phi^2 c_{\rm seg}$ with the third virial coefficient is negligible nearby the transition where $c_{\rm seg} \sim b_{\rm seg}^2 \sim 1$. For *intrachain* interactions the mentioned limit of low concentrations is fulfilled as well owing to the coil *friability*. Indeed, according to equation (8) the grain concentration inside the coil $\phi_{\rm seg} \sim 1/\sqrt{N}$.

5. Summary

In summary, we have extended the basic concepts of polymer physics to chains formed out of dipolar grains and established an important role of the chain flexibility. We have revealed a very deep similarity between dipolar chains and polymer molecules, however this analogy is not full: both the systems are not equivalent to each other. In particular, the mean length of the dipolar chain is not an independent parameter—as it is in the case of polymer molecules—as it strongly depends on the coupling constant: $\langle N \rangle \sim \exp(\lambda)$ (see equation (2)). This prohibits an identification of both systems and impedes the direct transfer of properties of a polymer chain with dipolar segments [28] onto pure a dipolar chain. Actually, the dipolar polymer molecule is a coil at high temperatures ($\lambda \ll N$) and becomes rod-like at low temperatures ($\lambda \sim N$) [28]. As demonstrated above, the results for the dipolar chain are entirely *opposite*: the chain exists in the form of coil or globule until dipolar interactions are strong ($\lambda \gg 1$), while with an increase of temperature it 'melts' and ceases to exist when λ nears unity. This is because the dipole interactions are *alone* responsible for structural transformations as well as for the chain formation itself and their also length.

Acknowledgments

Financial support provided by the INTAS Grant 03-51-6064 is gratefully acknowledged. This work was also supported by the Russian Fund for Fundamental Research (Projects 02-03-33003 and 04-02-96028) and the Israeli Science Foundation (Grant 272/03).

Appendix

We give here the calculation of the dimer partition functions $Z_2(0)$ and $Z_2(\infty)$ in zero and infinite magnetic fields, respectively, as well as calculations of the correlations (5). To this end, let us make some important remarks.

Consider first the case of zero external field. In general we should distinguish the dimer partition functions of two types. One of them is the partition function $Z_2(0;\mathbf{e}_1)$ for the *fixed* orientation $\mathbf{e}_1$ of particle 1, where the first argument of Z_2 is the value of field. In fact $Z_2(0;\mathbf{e}_1)$ is the one-particle partition function, describing the states of grain 2 in the field of particle 1. The definition of $Z_2(0;\mathbf{e}_1)$ is

$$Z_2(0;\mathbf{e}_1)=\int' \exp\left\{\frac{m^2}{r^3k_{\mathrm{B}}T}(3(\mathbf{e}_1\cdot\mathbf{n})(\mathbf{e}_2\cdot\mathbf{n})-\mathbf{e}_1\cdot\mathbf{e}_2)\right\}\frac{\mathrm{d}\mathbf{e}_2}{4\pi}\frac{\mathrm{d}\mathbf{r}}{v}, \tag{A.1}$$

where the prime denotes the integration over half of a spherical layer in accordance with the chain definition given in section 2. Other words, the absolute value of displacement vector $\mathbf{r}$ of two grains satisfies the condition $d\leqslant r\leqslant(2\lambda)^{1/3}d$ and the angle between $\mathbf{e}_1$ and $\mathbf{r}$ takes the values from zero to $\pi/2$.

Another quantity is the usual dimer partition function $Z_2(0)$ [14], including the integration over *all* orientations of *both* grains

$$Z_2(0)=\frac{1}{2}\int \exp\left\{\frac{m^2}{r^3k_{\mathrm{B}}T}(3(\mathbf{e}_1\cdot\mathbf{n})(\mathbf{e}_2\cdot\mathbf{n})-\mathbf{e}_1\cdot\mathbf{e}_2)\right\}\frac{\mathrm{d}\mathbf{e}_1}{4\pi}\frac{\mathrm{d}\mathbf{e}_2}{4\pi}\frac{\mathrm{d}\mathbf{r}}{v}. \tag{A.2}$$

We emphasize that here the orientations $\mathbf{e}_1$ and $\mathbf{e}_2$ are within the full angular-phase space volume equal to 4π and the coordinate integration is over the *whole* spherical layer $d\leqslant r\leqslant(2\lambda)^{1/3}d$.

Since in the case of zero field there is no preferable direction in the system, the integrals in (A.1) and (A.2) depend only on relative orientations $\mathbf{e}_1$ with $\mathbf{e}_2$ and $\mathbf{e}_1$ with $\mathbf{r}$. Therefore the result of (A.1) is independent of $\mathbf{e}_1$ and the integration over $\mathbf{e}_1$ in (A.2) reduces to the factor 4π. Thus both partition functions coincide with each other; $Z_2(0;\mathbf{e}_1)=Z_2(0)$.

We note that the dimer partition function $Z_2(0)$ is close to the usual second virial coefficient of two dipoles:

$$\begin{aligned} b_2&=-\frac{1}{2}\int\left[\exp\left\{-\frac{U(12)}{k_{\mathrm{B}}T}\right\}-1\right]\frac{\mathrm{d}\mathbf{e}_1}{4\pi}\frac{\mathrm{d}\mathbf{e}_2}{4\pi}\frac{\mathrm{d}\mathbf{r}}{v}\\ &=4-\frac{1}{2}\int\left[\exp\left\{\frac{m^2}{r^3k_{\mathrm{B}}T}(3(\mathbf{e}_1\cdot\mathbf{n})(\mathbf{e}_2\cdot\mathbf{n})-\mathbf{e}_1\cdot\mathbf{e}_2)\right\}-1\right]\frac{\mathrm{d}\mathbf{e}_1}{4\pi}\frac{\mathrm{d}\mathbf{e}_2}{4\pi}\frac{\mathrm{d}\mathbf{r}}{v}. \end{aligned} \tag{A.3}$$

Here the dimensionless value b_2 is given in units of particle volume v and $U(12)$ is the potential (1). After extracting the contribution of steric interactions given by 4, the integration is fulfilled over $r>d$. It is obvious that absolute values of both quantities coincide with each other in the limit of large λ.

Let us calculate now the dimer partition function $Z_2(0)$ (see equation (A.2)). After trivial integration over $\mathbf{e}_1$, resulting in factor 4π, we chose this vector as a polar axis. Now we have to calculate the integral of five variables, including two angles (polar and azimuthal) of vector $\mathbf{e}_2$,

two angles of orientation $\mathbf{n} = \mathbf{r}/r$ and a space variable r. The integration over three angular variables is elementary. The result is

$$Z_2(0) = \frac{4\pi}{v}\int_d^{(2\lambda)^{1/3}d} r^2\,\mathrm{d}r\int_0^1 \mathrm{d}x\,\frac{\sinh[\tilde{\lambda}(1-3x^2)/2]}{\tilde{\lambda}(1-3x^2)}I_0[3\tilde{\lambda}(1-x^2)/2], \tag{A.4}$$

where I_0 is the modified Bessel function of zero order and $\tilde{\lambda} = m^2/r^3k_\mathrm{B}T$. Changing variable $r \to \tilde{\lambda}$ and substituting $v = \pi d^3/6$, we find

$$Z_2(0) = 8\lambda\int_{0.5}^{\lambda}\frac{\mathrm{d}\tilde{\lambda}}{\tilde{\lambda}^3}\int_0^1 \mathrm{d}x\,\frac{\sinh[\tilde{\lambda}(1-3x^2)/2]}{1-3x^2}I_0[3\tilde{\lambda}(1-x^2)/2]. \tag{A.5}$$

The expression of the second virial coefficient b_2 is similar to equation (A.5), namely

$$b_2 = 4 - 8\lambda\int_0^{\lambda}\frac{\mathrm{d}\tilde{\lambda}}{\tilde{\lambda}^3}\int_0^1 \mathrm{d}x\,\left\{\frac{\sinh[\tilde{\lambda}(1-3x^2)/2]}{1-3x^2}I_0[3\tilde{\lambda}(1-x^2)/2] - \frac{\tilde{\lambda}}{2}\right\}. \tag{A.6}$$

In the limit of *small* λ it reproduces the well-known result of the paper by Joslin [29]:

$$b_2 = 4\left(1 - \tfrac{1}{3}\lambda^2 - \tfrac{1}{75}\lambda^4 - \tfrac{29}{55\,125}\lambda^6 - \tfrac{11}{694\,575}\lambda^8 - \mathrm{O}(\lambda^{10})\right). \tag{A.7}$$

Here and below we used the package Maple V in the calculational work. Analogous series over powers of dipolar parameter can be written for $Z_2(0)$. Our aim however is to analyse the opposite case of high values of λ, i.e. the determination of asymptotic behaviour of functions. For that we expand first functions $\sinh(y)$ and $I_0(y)$ in equation (A.5) into asymptotic series of high values of argument y. Then the straightforward integration gives the result (3). To conclude the discussion of calculation of $Z_2(0)$ we note that its small λ expansion describes perfectly the function behaviour in the whole region $0.5 \leqslant \lambda \leqslant 10$ when retaining terms up to $\sim\lambda^{20}$. Nevertheless the values of $Z_2(0)$ depicted in figure 1 were found directly from equation (A.5) by numerical calculations.

The calculation of the dimer partition function in infinite external field $Z_2(\infty)$ is simpler. Now all dipoles are along the field and

$$Z_2(\infty) = \frac{1}{2}\int \exp\left\{\frac{m^2}{r^3k_\mathrm{B}T}(3\cos^2\theta - 1)\right\}\frac{\mathrm{d}\mathbf{r}}{v}, \tag{A.8}$$

where θ is the angle between the displacement vector $\mathbf{r}$ and external field $\mathbf{H}$. The changing of variables reduces this relation to

$$Z_2(\infty) = 4\lambda\int_{0.5}^{\lambda}\frac{\mathrm{d}\tilde{\lambda}}{\tilde{\lambda}^2}\int_0^1 \mathrm{d}x\,\mathrm{e}^{3\tilde{\lambda}x^2}. \tag{A.9}$$

The calculated values of $Z_2(\infty)$ are shown in figure 1. The asymptotic expansion (4) follows immediately from equation (A.9).

Calculate now the averages in (5). Averaging in these expressions, the orientation $\mathbf{e}_1$ of the first grain is assumed to be fixed and taken as a polar axis. Then the mean cosine $A = (\mathbf{e}_1 \cdot \mathbf{e}_2)$ is equal in zero field

$$A = \frac{\int' \exp(-U_{dd}/k_\mathrm{B}T)\,(\mathbf{e}_1 \cdot \mathbf{e}_2)\,\mathrm{d}\mathbf{e}_2\,\mathrm{d}\mathbf{r}}{4\pi v Z_2(0;\,\mathbf{e}_1)}, \tag{A.10}$$

where U_{dd} is the dipolar part of potential (1). In complete analogy with the calculation of the partition function $Z_2(0)$ we have

$$A = \frac{8\lambda}{Z_2(0)}\int_{0.5}^{\lambda}\frac{\mathrm{d}\tilde{\lambda}}{\tilde{\lambda}^3}\int_0^1 \mathrm{d}x\,\frac{\sinh\left[\frac{\tilde{\lambda}}{2}(1-3x^2)\right]}{1-3x^2}L\left[\frac{\tilde{\lambda}}{2}(1-3x^2)\right]I_0\left[\frac{3}{2}\tilde{\lambda}(1-x^2)\right], \tag{A.11}$$

where $L(y) = \coth(y) - 1/y$ is the Langevin function. From here it is easy to find an expansion of A for small λ. The calculation of asymptotic expansion is analogous to that for $Z_2(0)$. The final result is

$$A = 1 - \frac{2}{\lambda} - \frac{2}{\lambda^2} - \frac{20}{3\lambda^3} - \frac{266}{9\lambda^4} - \frac{4241}{27\lambda^5} - \frac{77\,669}{81\lambda^6}. \tag{A.12}$$

Consider now the average value of $B = \langle \mathbf{e}_1 \cdot \mathbf{r}_{12} \rangle d^{-1}$. As in the previous case (cf (A.10)), we have

$$B = \frac{\int' \exp(-U_{dd}/k_{\mathrm{B}}T)\,(\mathbf{e}_1 \cdot \mathbf{r}_{12})\,\mathrm{d}\mathbf{e}_2\,\mathrm{d}\mathbf{r}}{4\pi\, dv\, Z_2(0; \mathbf{e}_1)}. \tag{A.13}$$

In as much as the angle between $\mathbf{e}_1$ and $\mathbf{r}_{12}$ is assumed to vary from zero to $\pi/2$, the integrand function in (A.13) takes positive values resulting in a non-zero value of B. The analytic representation of B proves to be the simplest among all correlations (5):

$$B = \frac{4\lambda^{4/3}}{3Z_2(0)} \int_{0.5}^{\lambda} \frac{\cosh 2\tilde{\lambda} - \cosh \tilde{\lambda}}{\tilde{\lambda}^{13/3}}\,\mathrm{d}\tilde{\lambda}. \tag{A.14}$$

From here the asymptotic expansion for $\lambda \gg 1$ follows:

$$B = 1 - \frac{1}{2\lambda} - \frac{5}{9\lambda^2} - \frac{11}{6\lambda^3} - \frac{689}{81\lambda^4} - \frac{15\,593}{324\lambda^5} - \frac{229\,265}{729\lambda^6}. \tag{A.15}$$

The other averages C, D, E and F can be calculated in the same way. We indicate only their analytic representations. The expression for C looks like (A.11) with a single difference: instead of L it contains $L^2 + L'$, where L' is the derivative of the Langevin function. The average D is equal

$$D = \frac{4\lambda^{5/3}}{Z_2(0)} \int_{0.5}^{\lambda} \frac{\mathrm{d}\tilde{\lambda}}{\tilde{\lambda}^{11/3}} \int_0^1 \mathrm{d}x\, \frac{1 - x^2}{1 - 3x^2}\,[I_0(z) + I_1(z)L(y)] \sinh y, \tag{A.16}$$

where I_1 is the modified Bessel function of first order and we use for short the notation $y = \tilde{\lambda}(1 - 3x^2)/2$ and $z = 3\tilde{\lambda}(1 - x^2)/2$.

The averages E and F are similar to (A.5) and can be written both as a function of parameter n

$$G(n) = \frac{8\lambda^{1+(n+1)/3}}{Z_2(0)} \int_{0.5}^{\lambda} \frac{\mathrm{d}\tilde{\lambda}}{\tilde{\lambda}^{2+(n+1)/3}} \int_0^1 \mathrm{d}x\, \frac{\sinh y}{1 - 3x^2} I_0(z). \tag{A.17}$$

The values of E and F are found from here for $n = 1$ and 2, respectively.

The asymptotic expansions of the correlations C, D, E and F are

$$C = 1 - \frac{4}{\lambda} + \frac{4}{\lambda^2} + \frac{8}{3\lambda^3} + \frac{74}{9\lambda^4} + \frac{998}{27\lambda^5} + \frac{16\,880}{81\lambda^6}, \tag{A.18}$$

$$D = 1 - \frac{1}{\lambda} - \frac{7}{18\lambda^2} - \frac{43}{27\lambda^3} - \frac{397}{54\lambda^4} - \frac{20\,185}{486\lambda^5} - \frac{398\,579}{1458\lambda^6}, \tag{A.19}$$

$$E = 1 + \frac{1}{6\lambda} + \frac{4}{9\lambda^2} + \frac{44}{27\lambda^3} + \frac{1175}{162\lambda^4} + \frac{18\,007}{486\lambda^5} + \frac{153\,715}{729\lambda^6}, \tag{A.20}$$

$$F = 1 + \frac{1}{3\lambda} + \frac{17}{18\lambda^2} + \frac{97}{27\lambda^3} + \frac{2657}{162\lambda^4} + \frac{41\,507}{486\lambda^5} + \frac{719\,573}{1458\lambda^6}. \tag{A.21}$$

So, we determined the asymptotic representations at $\lambda \gg 1$ of the orientational and spatial dimer correlations (5) for zero external field. The calculation for the case of infinite field is much simpler than mentioned above and we omit it. We point out that the dimer correlations

A_∞ and C_∞ are obviously equal to unity, because two dipoles in infinite field are aligned along field direction. The averages left have a form

$$B_\infty = 1 + \frac{7}{36\lambda^2} + \frac{25}{36\lambda^3} + \frac{1787}{648\lambda^4} + \frac{1000}{81\lambda^5} + \frac{715\,597}{11\,664\lambda^6}, \tag{A.22}$$

$$D_\infty = 1 + \frac{4}{9\lambda^2} + \frac{85}{54\lambda^3} + \frac{343}{54\lambda^4} + \frac{56\,255}{1944\lambda^5} + \frac{106\,571}{729\lambda^6}, \tag{A.23}$$

$$E_\infty = 1 + \frac{1}{6\lambda} + \frac{13}{36\lambda^2} + \frac{119}{108\lambda^3} + \frac{2675}{648\lambda^4} + \frac{34\,801}{1944\lambda^5} + \frac{508\,025}{5832\lambda^6}, \tag{A.24}$$

$$F_\infty = 1 + \frac{1}{3\lambda} + \frac{7}{9\lambda^2} + \frac{67}{27\lambda^3} + \frac{3109}{324\lambda^4} + \frac{10\,366}{243\lambda^5} + \frac{2472\,103}{11\,664\lambda^6}. \tag{A.25}$$

References

[1] Shliomis M I 1974 *Usp. Fiz. Nauk* **112** 427
Shliomis M I 1974 *Sov. Phys.—Usp.* **17** 153 (Engl. Transl.)
[2] Rosensweig R E 1985 *Ferrohydrodynamics* (Cambridge: Cambridge University Press)
[3] Weis J J and Levesque D 1993 *Phys. Rev. Lett.* **71** 2729
[4] Caillol J M 1993 *J. Chem. Phys.* **98** 9835
[5] van Leeuwen M E and Smit B 1993 *Phys. Rev. Lett.* **71** 3991
[6] Stevens M J and Grest G S 1994 *Phys. Rev. Lett.* **72** 3686
[7] Levesque D and Weis J J 1994 *Phys. Rev.* E **49** 5131
[8] Morozov K I, Pshenichnikov A F, Raikher Yu L and Shliomis M I 1987 *J. Magn. Magn. Mater.* **65** 173
[9] Wertheim M S 1971 *J. Chem. Phys.* **55** 4291
[10] Camp P J, Shelley J C and Patey G N 2000 *Phys. Rev. Lett.* **84** 115
[11] ten Wolde P R, Oxtoby D W and Frenkel D 1998 *Phys. Rev. Lett.* **81** 3695
[12] ten Wolde P R, Oxtoby D W and Frenkel D 1999 *J. Chem. Phys.* **111** 4762
[13] de Gennes P G and Pincus P A 1970 *Phys. Kondens. Mater.* **11** 189
[14] Jordan P C 1973 *Mol. Phys.* **25** 961
[15] van Roij R 1996 *Phys. Rev. Lett.* **76** 3348
[16] Sear R P 1996 *Phys. Rev. Lett.* **76** 2310
[17] Levin Y 1999 *Phys. Rev. Lett.* **83** 1159
[18] Osipov M A, Teixeira P I C and Telo da Gama M M 1996 *Phys. Rev.* E **54** 2597
[19] Tavares J M, Telo da Gama M M and Osipov M A 1997 *Phys. Rev.* E **56** R6252
[20] Tavares J M, Weis J J and Telo da Gama M M 1999 *Phys. Rev.* E **59** 4388
[21] Zubarev A Yu and Iskakova L Yu 1995 *JETP* **80** 857
[22] Zubarev A Yu and Iskakova L Yu 2000 *Phys. Rev.* E **61** 5415
[23] Grosberg A Yu and Khokhlov A R 1994 *Statistical Physics of Macromolecules* (New York: American Institute of Physics)
[24] Fisher M E 1964 *Am. J. Phys.* **32** 343
[25] Ivanov A O and Kuznetsova O B 2001 *Phys. Rev.* E **64** 041405
[26] Kirkwood J G 1939 *J. Chem. Phys.* **7** 911
[27] Camp P J and Patey G N 2000 *Phys. Rev.* E **62** 5403
[28] Muthukumar M 1996 *J. Chem. Phys.* **104** 691
[29] Joslin C G 1981 *Mol. Phys.* **42** 1507